Cancer Research

Accumulation of Multipotent Progenitors with a Basal Differentiation Bias during Aging of Human Mammary Epithelia

James C. Garbe, Francois Pepin, Fanny A. Pelissier, et al.

Updated version	Access the most recent version of this article at: doi:10.1158/0008-5472.CAN-12-0157
Supplementary Material	Access the most recent supplemental material at: http://cancerres.aacrjournals.org/content/suppl/2012/04/27/0008-5472.CAN-12-0157.DC1.html

Cited Articles	This article cites by 48 articles, 13 of which you can access for free at: http://cancerres.aacrjournals.org/content/72/14/3687.full.html#ref-list-1

E-mail alerts	Sign up to receive free email-alerts related to this article or journal.
Reprints and Subscriptions	To order reprints of this article or to subscribe to the journal, contact the AACR Publications Department at pubs@aacr.org.
Permissions	To request permission to re-use all or part of this article, contact the AACR Publications Department at permissions@aacr.org.

Tumor and Stem Cell Biology

Accumulation of Multipotent Progenitors with a Basal Differentiation Bias during Aging of Human Mammary Epithelia

James C. Garbe[1], Francois Pepin[1], Fanny A. Pelissier[1,4], Klara Sputova[1], Agla J. Fridriksdottir[2], Diana E. Guo[1], Rene Villadsen[2], Morag Park[3], Ole W. Petersen[2], Alexander D. Borowsky[5], Martha R. Stampfer[1], and Mark A. LaBarge[1]

Abstract

Women older than 50 years account for 75% of new breast cancer diagnoses, and the majority of these tumors are of a luminal subtype. Although age-associated changes, including endocrine profiles and alterations within the breast microenvironment, increase cancer risk, an understanding of the cellular and molecular mechanisms that underlies these observations is lacking. In this study, we generated a large collection of normal human mammary epithelial cell strains from women ages 16 to 91 years, derived from primary tissues, to investigate the molecular changes that occur in aging breast cells. We found that in finite lifespan cultured and uncultured epithelial cells, aging is associated with a reduction of myoepithelial cells and an increase in luminal cells that express keratin 14 and integrin-α6, a phenotype that is usually expressed exclusively in myoepithelial cells in women younger than 30 years. Changes to the luminal lineage resulted from age-dependent expansion of defective multipotent progenitors that gave rise to incompletely differentiated luminal or myoepithelial cells. The aging process therefore results in both a shift in the balance of luminal/myoepithelial lineages and to changes in the functional spectrum of multipotent progenitors, which together increase the potential for malignant transformation. Together, our findings provide a cellular basis to explain the observed vulnerability to breast cancer that increases with age. *Cancer Res; 72(14); 3687–701. ©2012 AACR.*

Introduction

The frequency of human carcinomas increases with age, and the dominant paradigm suggests that acquired mutations and epigenetic modifications account for that increase (1). The vast majority of women (>75%) diagnosed with breast cancer are older than 50 years (2, 3), and those tumors are largely of a luminal subtype (4). Although a few mutations are specifically associated with breast cancers, there does not appear to be a strong age-dependent association with particular mutations (5). Age-related changes in epigenetic modifications, such as DNA methylation, have been reported in a number of different tumors (6, 7). An age-dependent, estrogen receptor–independent gene expression signature identified in type-matched

breast tumors (5) also suggests that epigenetic and/or micro-environmental changes are involved in the pathogenesis of age-related breast cancers. However, at present, there is not striking genetic or epigenetic evidence that fully explains the increased incidence of breast cancer with advanced age.

Changes in endocrine regulation and in the cellular and molecular composition of breast microenvironment are the foremost factors that a majority of women aged over 50 years have in common. The timing of changes in the endocrine system associated with menopause is correlated with the physical changes in breast composition, although mechanisms are unknown. Estrogen and progesterone can directly impact the epithelium by causing fluctuations in the stem cell pool (8, 9) and are required for gland morphogenesis (10–12). The effects of cyclic and prolonged exposures of the normal epithelium to sex hormones over a lifespan are not well defined, although it is known that hormone replacement therapy can induce a higher risk of breast cancer (13, 14). Aging also is associated with physical changes to the breast such as increases in adipose cells and decreased overall density (15, 16). Changes in protease expression (17) could be related to age-related discontinuities in laminin-111 of the basement membrane (18), which could impact tissue polarity (19). These changes occur gradually, thus slowly evolving the molecular constituency of the breast microenvironment. Microenvironmental composition was shown to skew the fate decision process in human mammary multipotent progenitors (20).

Authors' Affiliations: [1]Life Science Division, Lawrence Berkeley National Laboratory, Berkeley, California; [2]Department of Cellular and Molecular Medicine, Centre for Biological Disease Analysis and Danish Stem Cell Centre, Faculty of Health Sciences, University of Copenhagen, Denmark; [3]Department of Biochemistry, McGill University, Rosalind and Morris Goodman Cancer Centre, Montreal, Canada; [4]Institute of Bioengineering, Ecole Polytechnique Fédérale de Lausanne, Lausanne, Switzerland; and [5]Department of Pathology, University of California Davis, Sacramento, California

Corresponding Author: Mark A. LaBarge, Lawrence Berkeley National Laboratory, 1 Cyclotron Road, MS977, Berkeley CA 94720. Phone: 510-486-4544; Fax: 510-486-5568; E-mail: MALabarge@lbl.gov

American Association for *Cancer Research*

Thus, age-related changes to microenvironment could affect the differentiation and proportion of epithelial lineages.

Changes to the balance of human mammary epithelial cell (HMEC) lineages in the epithelium may presage susceptibility to breast cancer. Loss of the myoepithelial lineage is linked to breast cancer progression, possibly because they produce laminin-111, which is a key basement membrane component that maintains normal polarity (19, 21). Humans and mice bearing *BRCA-1* mutations exhibited increased proportions of putative luminal progenitors that correlated with increased cancer risk (22–24). In MMTV-PyMT transgenic mice, which are models of Her2-positive luminal-type tumors, the numbers of progenitors increased in a tumor stage–specific manner, suggesting they may play a role in luminal breast cancer pathogenesis as well (25). Tumors that are thought to arise due to mutations in BRCA-1 account for only about 5% of all breast cancers, whereas age-related breast cancers account for more than 75% of all cases. Given growing support for an etiologic relationship between changes in the progenitors of normal mammary epithelia and cancer progression, it is important to determine the impact of aging on progenitors and more committed lineages of the human mammary epithelium. Herein, we reveal fundamental age-dependent transcriptional and functional changes to HMECs that are associated with changes in the distributions of luminal, myoepithelial, and multipotent progenitors, which together provide a cellular basis for increased vulnerability to breast cancer with age.

Materials and Methods

Cell culture

HMEC strains were established and maintained according to previously reported methods (26) using M87A medium with oxytocin and cholera toxin (27). For 3-dimensional (3D) cultures, a feeder layer of unsorted primary epithelial cells was made in 24-well plates. Two hundred and fifty microliters of growth factor–reduced Matrigel (Becton Dickinson) was then layered on top of the feeder layer and allowed to polymerize at 37°C. Ten thousand fluorescence-activated cell-sorting (FACS)-enriched cells were resuspended in 300 to 350 μL of Matrigel and then layered on top of the cell-free gel and then polymerized at 37°C. Gels were cultured with H14 medium.

Flow cytometry

HMECs at fourth passage were trypsinized and resuspended in their media. For enrichment or identification of luminal epithelial and myoepithelial lineages, anti-CD227-FITC (Becton Dickinson, clone HMPV) or anti-CD10-PE, -PE-Cy5 or -APC (BioLegend, clone HI10a), respectively, or of LBP, anti-CD117-Alexa647 (BioLegend, clone 104D2), EpCam-BV421 (BioLegend, clone 9C4) were added to the media at 1:50 for 25 minutes on ice, washed in PBS, and sorted or analyzed. Anti-CD49f-PE (Chemicon, clone CBL-458P) was used at 1:100 dilution. Results were consistent across multiple instrumentation platforms: at LBNL, FACSCalibur (Becton Dickinson) for analysis only and FACS Vantage DIVA (Becton Dickinson) for sorting at LBNL and a FACSAria (Becton Dickinson) at University of Copenhagen (Copenhagen, Denmark).

Immunofluorescence and immunohistochemistry

Cultured HMECs were fixed in methanol:acetone (1:1) at −20°C for 15 minutes, blocked with PBS/5% normal goat serum/0.1% Triton X-100, and incubated with anti-K14 (1:1,000, Covance, polyclonal rabbit) and anti-K19 (1:20, Developmental Studies Hybridoma Bank, clone Troma-III) overnight at 4°C, then visualized with fluorescent secondary antibodies (Invitrogen). 5-ethynyl-2′-deoxyuridine (EdU) was added to culture media 4 hours before harvesting cells for immunofluorescence and was imaged with A647 click reagents according to manufacturer's specifications (Invitrogen). Cells were imaged with a 710LSM microscope (Carl Zeiss). Four-color image analysis of K14, K19, EdU, and 4′,6-diamidino-2-phenylindole (DAPI) was conducted using a modified watershed method in MatLab software (MathWorks).

Paraffin-embedded tissue sections were deparaffinized and antigen-retrieved (Vector Labs). For immunofluorescence, sections were blocked and stained as above. Primary antibodies used were K14 as above, K19 (1:100, AbCam, AAH07628), and K8 was visualized with anti K8 (1:100, AbCam, clone HK-8). For immunohistochemistry, a Dako Autostainer was used together with all Dako reagents for staining. Samples were blocked in Dual Endogenous Enzyme; EnVision+ Dual Link System-HRP was used as the secondary antibody (Dako). Liquid DAB+ Substrate Chromogen System was used as the substrate (Dako). Nuclei were stained with hematoxylin. Sections were incubated with the following primary antibodies for 20 to 30 minutes at room temperature: CD10 [ready to use (RTU), Leica, clone56C6], CD117 (1:600, Dako, polyclonal), K5/6 (RTU, Dako, D5/16B4), K19 (RTU, Dako, RCK108), and HMA (1:200, Dako, HHF35).

Gene expression analysis

Expression profiles of morphologically normal human epithelial cells were obtained as described previously (28). Expression profiles for pre-stasis HMECs at multiple passages were obtained as described previously (27).

Differential expression was conducted using R/Bioconductor using the LIMMA method (29). A gene is considered differentially expressed if the P value adjusted by the Benjamini–Hochberg (30) false discovery rate (FDR) method is <0.01 for the laser capture microdissected (LCM) samples and 0.1 for the cell lines. A more stringent threshold is used in the case of the cell strains because of the increased power associated with the larger sample size. In the case of the microdissected profiles, cells from women younger than 45 years ($n = 17$) were compared with cells from women ages 60 years or older. In the case of the cell strains, the earliest passage (passage 2) for each strain was used. The 3 cell strains from women younger than 30 years (184D, 48R, and 240L) were compared with 3 strains from women older than 55 years (122L, 153L, and 96R).

Cross-platform comparison was done using the HUGO gene symbols contained in the annotations of the R/Bioconductor packages hgu133a2.db and hgug4112a.db version 2.4.5. Enrichment was conducted using Fisher exact test based on the total number of differentially expressed probes associated
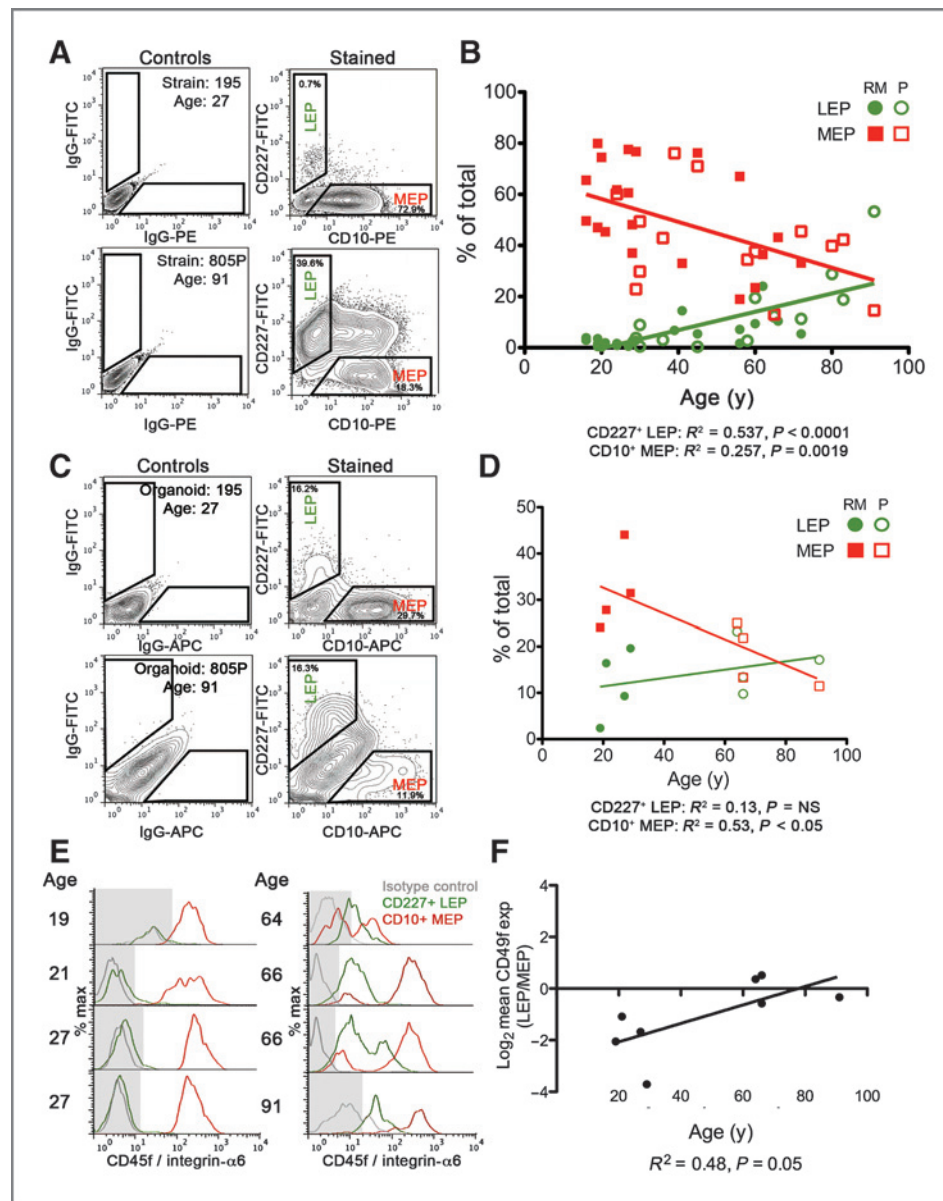
Figure 1. Epithelial lineages change as a function of age. A, representative FACS analyses of CD227 and CD10 expression in fourth-passage HMEC strains isolated from one woman younger than 30 years (195L) and one older than 55 years (805P). FACS plots are shown as 5% contour plots with outliers identified; left, isotype antibody controls; right, the CD10- and CD227-stained samples. Gates identifying luminal epithelial (LEP) and myoepithelial (MEP) are shown. FITC, fluorescein isothiocyanate; PE, phycoerythrin. B, linear regression showing changes in proportions of LEPs (green) and MEPs (red) in HMEC strains at fourth passage as a function of age ($n = 36$ individuals). LEPs and MEPs from reduction mammoplasty (RM)-derived strains are shown with filled circles or boxes and from peripheral to tumor (P)-derived strains with open circles or boxes, respectively. C, representative FACS analyses from the corresponding uncultured dissociated epithelial organoids. FACS plots are shown as 5% contour plots with outliers identified; left, isotype antibody controls; right, the CD10- and CD227-stained samples. APC, allophycocyanin. D, linear regression of proportions of LEPs (green) and MEPs (red) in dissociated uncultured organoids as a function of age ($n = 8$ individuals). LEPs and MEPs from RM-derived organoids are shown with filled circles or boxes, and from P-derived organoids with open circles or boxes, respectively. NS, not significant. E, histograms of CD49f (integrin-α6) expression by flow cytometry on CD227+ LEPs (green lines) and CD10+ MEPs (red lines) from dissociated organoids. The gray-colored shade boxes indicate the threshold at which there is little or no CD49f expression as determined in isotype negative control stains (gray lines). F, regression analysis of log$_2$ change in mean expression of CD49f in LEPs normalized to the levels in MEPs from dissociated organoids as a function of age ($n = 8$ individuals).

with HUGO gene symbols. To facilitate the cross-platform comparison in Fig. 1D and E; Supplementary Fig. S1, only the top 100 unique genes from the LCM represented on both platforms were used. In the Agilent platform, only the probe

with the lower P value was used if several probes mapped to the same gene. In the Affymetrix platform, the probe set with the highest variance is selected. Accession number for GEO database is GSE37485.

Statistical analysis

GraphPad Prism 5.0 was used for all statistical analysis, with exception of gene expression analysis (see above). One-way ANOVA were used for all data sets. Linear regression was used to determine changes as a function of age, significance was established when $P < 0.05$. Grouped analyses were conducted with Boneferroni test for multiple comparisons and Bartlett test for equal variance, with significance established when $P < 0.05$.

Results

Myoepithelial cells decline, and luminal cells become more numerous and more basal-like with age

We generated a diverse cohort of finite lifespan HMEC strains to facilitate functional analysis of the aging process in humans. This HMEC Aging Resource was derived from a collection of uncultured organoids from more than 200 individuals aged 16 to 91 years. Organoids from 36 reduction mammoplasty and peripheral nontumor mastectomy tissues (Table 1) were cultured using low-stress medium, M87A with oxytocin (27). M87A medium supports growth of multiple mammary epithelial lineages for up to 40 to 60 population doublings before stasis, a stress-associated senescence arrest (27). In contrast, the defined serum-free MCDB170-type media, such as the commercially sold MEGM, support $p16^{INK4A}(-)$ post-stasis HMEC with basal or myoepithelial phenotypes, and a greatly reduced pre-stasis proliferative potential (refs. 31, 32; Supplementary Fig. S1A).

Comparative phenotypic and molecular analyses revealed that pre-stasis HMEC strains retained the same lineages present *in vivo*. Flow cytometric (FACS) analyses of dissociated mammary epithelial organoids using antibodies that recognized luminal epithelial and myoepithelial lineage markers (CD227 and CD10, respectively; ref. 33), showed the presence of both lineages (Supplementary Fig. S1B, left). Pre-stasis cultures were initiated from undissociated organoids attached to tissue culture plastic (26). Immunofluorescent analysis of keratin intermediate filament proteins (K)14 and K19 verified that $K14^+/K19^-$ myoepithelial, $K14^-/K19^+$ luminal epithelial, and $K14^+/K19^+$ putative progenitors (34, 35) were present in HMEC populations that migrated onto and proliferated on the culture plastic (Supplementary Fig. S1B, right). All experiments reported here that involved cultured strains were carried out on fourth-passage pre-stasis HMECs because they were found to be heterogeneous; luminal epithelials (0.5% to 53% of total) and myoepithelials (14% to 97%) were present in every pre-stasis strain at fourth passage (for example, see Supplementary Fig. S1C). Comparison of HMEC lineage markers in 2 fourth-passage strains and 2 uncultured dissociated organoids using 7-parameter flow cytometry revealed that the $CD10^-/CD227^+$ luminal epithelials correspond to the $EpCam^{hi}/CD49f^{low}$ population and the $CD10^+/CD227^-$ myoepithelials correspond to the $EpCam^{low}/CD49f^{hi}$ population (Supplementary Fig. S3). When using flow cytometry, luminal epithelial and myoepithelial lineages were principally defined using CD10 and CD227 in this study because the distribution of the cells expressing those 2 markers in fourth-passage HMEC

more closely reflected the distribution observed in primary dissociated organoids, whereas the distributions of EpCam and CD49f expression changed slightly because of culture adaptation.

Lobules involute with advancing age leaving behind ducts and residual lobules with changed morphology (15, 36), suggesting that representation of luminal epithelials, myoepithelials, and progenitors may change with age. FACS analyses of the 36 HMEC strains revealed that $CD227^-/CD10^+$ myoepithelial decreased ($P = 0.0019$) and that $CD227^+/CD10^-$ luminal epithelial increased ($P < 0.0001$) as proportions of the total population with age (Fig. 1A and B). We hypothesized that the age-dependent changes arose either through age-dependent shifts in the proportions of luminal epithelials and myoepithelials in the organoids used to establish the strains and/or through intrinsic changes to functional properties of luminal epithelials or myoepithelials that would aid survival or propagation of one lineage. Examination by FACS of 8 uncultured organoids, which were dissociated in parallel, revealed that myoepithelial proportions decreased ($P < 0.05$) and proportions of luminal epithelials trended upward with age (Fig. 1C and D). Evidence of age-dependent functional changes in luminal epithelials that could alter their ability to bind extracellular matrix (ECM) and survive in culture was observed by FACS measurement of CD49f (integrin-α6) protein expression, which is used by myoepithelials to attach to the basement membrane. CD49f was increasingly expressed in luminal epithelials from uncultured organoids as a function of age ($P = 0.05$), reaching a level on a par with the myoepithelials from the same specimen (Fig. 1E and F). Whereas luminal epithelials and myoepithelials from women younger than 30 years showed unimodal distributions of CD49f expression, bimodal distributions of CD49f expression were measured in myoepithelials in 3 of 4, and in 1 of 4 luminal epithelial specimens in the above 55-year group, suggesting that aging was associated with evolution of additional lineage subsets not present in younger women (Fig. 1E). Thus, a decline of myoepithelials and an increase of luminal epithelials that exhibited molecular features usually ascribed to myoepithelials were measured with increasing age in cultured pre-stasis strains and in cells from uncultured dissociated organoids.

Age-dependent gene expression hallmarks from *in vivo* are preserved in pre-stasis HMEC strains

To determine whether molecular hallmarks of aging *in vivo* were preserved in cultured HMEC strains, gene expression patterns from HMEC strains (three <30 years and three >55 years) were compared with gene expression patterns from LCM morphologically normal breast epithelium from 59 individuals ages 27 to 77 years undergoing reduction mammoplasty or cancer removal surgery (28). In the LCM data set, 3,013 unique genes were differentially expressed (FDR < 0.05; LIMMA; ref. 29) between women younger than 45 years and 60 years or above. The top 100 differentially expressed genes stratified the entire collection of LCM samples as a function of age (Fig. 2A). Analysis of 6 HMEC strains identified 121 unique differentially expressed genes between young and old. There is a significant overlap of 18 genes (*C2orf55, CCDC47,*

CLDN8, CREBBP, GFER, GRIN1, HCG26, IGF1, LEF1, MAN1A2, NPEPPS, PLEKHA1, PSD, SOCS3, SRSF10, STRN3, TCP11L1, and TF) between both sets of genes ($P = 0.04$; Fisher's exact test). The 100 genes from the *in vivo* tissues clustered the 6 HMEC strains, with representatives of early and late passages for each, based on the age of the women (Fig. 2B). Consistent with increased proportions of luminal epithelials in strains from women older than 55 years, the gene profiles from EpCam-enriched luminal epithelials from a 19-year (strain 240L) and from milk-derived luminal cells (strain 250MK) clustered with the major branch that contained all the strains from women older than 55 years. The gene profiles from CD10-enriched cells from strain 240L clustered with some later passage strains, consistent with the tendency for HMEC strains to become enriched for basal cells with extended culture. Thus, despite the different sources of RNA and gene array platforms, cultured pre-stasis HMEC appeared to retain a molecular signature of aging that was identified *in vivo*.

cKit+ HMEC are putative multipotent progenitors that are more numerous with age

Changes in lineage proportions in fourth-passage strains and in organoids were consistent across the strains, although it also was evident that cell culture on plastic caused a selection bias for cells with basal features (i.e., myoepithelials). Whereas the proportion of luminal epithelials increased with donor age when viewed at fourth passage or in organoids, it decreased with passage in culture, the decrease becoming pronounced by eighth passage (Fig. 3A). The receptor tyrosine kinase cKit was postulated to be a marker of luminal progenitors in humans from gene array analyses (22), and empirical evidence in mice showed its expression on putative luminal progenitors (37). The proportion of cKit-expressing (cKit+) HMECs, measured with FACS, decreased with passage in pre-stasis strains (Fig. 3A). However, cKit+ HMECs increased as a function of age when measured at fourth passage (Fig. 3B) and in 11 dissociated primary reduction mammoplasty samples (Fig. 3C).

To determine whether cKit+ HMEC were capable of self-maintenance, fourth-passage HMECs were FACS-enriched for cKit expression (Fig. 3D) and then cultured for 3 additional passages to assess the resultant culture composition. FACS analysis of the eighth-passage cultures started from cKit+ HMEC (Fig. 3F) revealed 20-fold enrichment for CD227+/CD10− luminal epithelial ($P < 0.05$) and 2-fold for cKit-expressing cells ($P < 0.05$) compared with parallel cultures started with unsorted HMECs (Fig. 3E).

To investigate morphogenic capacity, primary cKit+ HMECs from dissociated organoids were embedded in laminin-rich ECM (lrECM) at low density. Compared with cKit− cells, cKit+ were 6-fold enriched in their ability to form terminal-duct lobular-like units (TDLU; Fig. 3G): 3% of cKit+ cells formed TDLUs compared with 0.5% of cKit− cells ($n = 3$ individuals). The cKit+-derived TDLUs were composed of K19+ luminal epithelials and K14+ myoepithelials (Fig. 3H). That cKit+ showed a limited ability to self-maintain gave rise to CD227+/CD10−/K19+ luminal epithelials and CD227−/CD10+/K14+ myoepithelials and was capable of clonal and robust morphologic activity in 3D lrECM supported the

hypothesis that cKit+ cells were progenitors capable of multi-lineage differentiation.

Similar behavior was exhibited by reduction mammoplasty- and peripheral nontumor mastectomy–derived HMECs

The population of women who undergo reduction mammoplasty procedures is skewed toward younger ages. Much of the material used to establish strains and for organoid analyses from women older than 60 years were from peripheral non-tumor mastectomy–derived samples (Table 1). Although peripheral nontumor mastectomy tissues were normal-appearing, there may have been field effects or microtumors that were not detected. Therefore, age-dependent lineage distributions were compared from reduction mammoplasty- and peripheral nontumor mastectomy–derived HMEC strains as independent groups. The 21 reduction mammoplasty–derived strains showed significantly decreased proportions of myoepithelial ($P < 0.05$) and increased luminal epithelial ($P < 0.003$) and cKit+ HMEC ($P < 0.05$) with age (Supplementary Fig. S2A). The 15 peripheral nontumor mastectomy–derived strains showed significantly increased luminal epithelial ($P < 0.0007$), a trend for increasing cKit+ HMECs ($P = 0.0507$), and no change in myoepithelials with age (Supplementary Fig. S2B). Given that the 36 HMEC strains analyzed in this report were derived from a genetically diverse collection of individuals with unknown parity and estrous status, the observed R^2 values (from 0.246 to 0.606) and P values (from 0.05 to <0.0001) suggest a remarkable relationship with effects from aging. Comparison of proportions of the 3 lineages in reduction mammoplasty- and peripheral nontumor mastectomy–derived strains grouped by similar age (24–29 years reduction mammoplasty vs. 24–30 years peripheral nontumor mastectomy, and 41–62 years reduction mammoplasty vs. 45–65 years peripheral nontumor mastectomy) also revealed no significant differences within the age groups (Supplementary Fig. S2C–S2F). Thus, we detected no statistically significant differences in age-grouped reduction mammoplasty- versus peripheral nontumor mastectomy–derived strains and lineage distributions in strains derived from either tissue source followed similar patterns with age.

cKit+ progenitors exhibit an age-dependent basal activity bias

To determine whether a differentiation bias arose in HMECs with age, unsorted HMECs and FACS-enriched cKit+ cells (Fig. 4A) from 10 women (five <30 years and five >55 years) were subjected to lineage-forming assays. Lineage analyses were conducted with markers that were different from the ones used to FACS-enrich the cells, plus a marker of DNA synthesis, to gain additional information. The ratios of K14 to K19 proteins expressed and EdU incorporation were measured in each cell using automated quantitative image analysis. After 48 hours of culture, unsorted HMECs from women younger than 30 years exhibited pronounced K14+/K19− myoepithelial populations and minor K14−/K19+ luminal epithelial and K14+/K19+ progenitor populations (Fig. 4B and D, top left). The less than 30-year cKit-enriched population gave rise to 3

Table 1. List of specimens: characteristics of HMEC strains and uncultured organoids

Sample	Age, y	Source	Country of surgery[a]	Est pre-stasis strain	Organoid analysis[b]	Known characteristics/ pathology notes
48R	16	RM	USA	Yes		African-American
160	16	RM	USA	Yes		
240	19	RM	USA	Yes		Mildly hyperplastic
404	19	RM	USA	No	CD10, CD227, CD49f	Minimal fibrocystic change
407P	19	P	USA	Yes		IDC, lymph node+, ER+, PR+
168R	19	RM	USA	Yes		African-American
D1	19	RM	DK	No	cKit	
399	20	RM	USA	Yes		Benign
356	21	RM	USA	Yes	CD10, CD227, CD49f	Normal
184	21	RM	USA	Yes		
1P	24	P	USA	Yes		IDC, lymph node−
97	27	RM	USA	Yes		
195L	27	RM	USA	Yes	CD10, CD227, CD49f	
123	27	RM	USA	Yes		African-American, mammary hyperplasis
400	27	RM	USA	No	CD10, CD227, CD49f	Mild ductal ectsia and mastitis
51L	28	RM	USA	Yes		Mild periductal mastitis (R+L), focal microcalcification (R.)
172L	28	RM	USA	Yes		Minimal phase of fibrocystic disease
D2	28	RM	DK	No	cKit	
124	29	RM	USA	Yes		
676P	29	P	USA	Yes		
42P	30	P	USA	Yes		IDC, lymph node−
1030P	30	P	USA	Yes		
D2	30	RM	DK	No	cKit	
D4	32	RM	DK	No	cKit	
D5	33	RM	DK	No	cKit	
D6	34	RM	DK	No	cKit	
90P	36	P	USA	Yes		BRCA-1 mut (185delAG)
D7	37	RM	DK	No	cKit	
100P	39	P	USA	Yes		Noninvasive ductal carcinoma, ER−, PR−
D8	41	RM	DK	No	cKit	
245AT	41	RM	USA	Yes		ATM heterozyote, tissue was clinically normal tissue
D9	44	RM	DK	No	cKit	
D10	44	RM	DK	No	cKit	
173P	45	RM	USA	Yes		IDC, ER−, PR−
D11	54	RM	DK	No	cKit	
191	56	RM	USA	Yes		Slight fibrocystic disease, hypertrophy, stromal fibrosis, and adenosis present in mammary parenchyma
117	56	RM	USA	Yes		Patchy stromal fibrosis (R.), fibrocystic disease (L.)

(Continued on the following page)

Table 1. List of specimens: characteristics of HMEC strains and uncultured organoids (Cont'd)

Sample	Age, y	Source	Country of surgery[a]	Est pre-stasis strain	Organoid analysis[b]	Known characteristics/ pathology notes
335P	58	P	USA	Yes		Infiltrating adenocarcinoma, ER+, PR+/−
153L	60	RM	USA	Yes		Benign fibrocystic disease
639P	60	P	USA	Yes		
122L	62	RM	USA	Yes		Fibrocystic disease, hypertrophy, apocrine metaplasia of ductal epithelium, cystic dilatia of ducts, and focal areas of intraductal hyperplasia
394P	64	P	USA	No	CD10, CD227, CD49f	IDC
881P	65	P	USA	Yes		
355P	66	P	USA	No	CD10, CD227, CD49f	Infiltrating adenocarcinoma
374P	66	P	USA	No	CD10, CD227, CD49f	Infiltrating adenocarcinoma, Padget disease
96R	66	RM	USA	Yes		Slight focal fibrocystic change
429	72	RM	USA	Yes		
353P	72	P	USA	Yes		Colloid (mucinous) carcinoma, ER+/−, PR−
464P	80	P	USA	Yes		
451P	83	P	USA	Yes		
805P	91	P	USA	Yes	CD10, CD227, CD49f	

NOTE: Known characteristics/pathology notes: information is incomplete but was provided for cases in which some outstanding feature was known to the authors or was noted in pathology reports.

Abbreviations: ER, estrogen receptor; IDC, invasive ductal carcinoma; P, peripheral nontumor containing mastectomy tissue; PR, progesterone receptor; RM, reduction mammoplasty tissue.

[a]Country of surgery: USA, Peralta Cancer Center, Oakland, California; DK, University of Copenhagen.

[b]Organoid analysis: anti-CD10 clone HI10a, anti-CD227 clone HMPV, anti-CD49f clone GoH3, anti-cKit clones 104D2 and K45.

distinct populations corresponding to luminal epithelial, progenitors, and myoepithelial, which is consistent with our interpretation of multipotent activity (Fig. 4B and D, top right). Unsorted HMEC from women older than 55 years exhibited a minor K14−/K19+ luminal epithelial population and pronounced K14+/K19+ progenitor and K14+/K19− myoepithelial populations (Fig. 4B and D, bottom left). Surprisingly, older than 55-year cKit-enriched population showed little evidence of differentiation into K14−/K19+ luminal epithelials, instead, exhibiting mainly a K14+/19+ phenotype (Fig. 4B and D, bottom right). Thus, older than 55-year cKit+ progenitors have a defect in differentiation, which makes them unable to produce CD227+/K14−/K19+ luminal epithelials in any significant proportion.

To determine whether HMEC lineages differed in their rate of proliferation as a function of age, the percentage of cells that incorporated EdU in unsorted and cKit+ HMEC was measured. In unsorted cultures, K14+ myoepithelials from women younger than 30 years incorporated significantly more EdU than less than 30-year K19+ luminal epithelials or K14+/K19+ progenitor cells, and more myoepithelials from older than 55-year HMEC strains ($P < 0.05$; Fig. 4C, top). All 3 lineages in strains from women older than 55 years exhibited similar levels of EdU incorporation, suggesting that there was no proliferative advantage for one lineage over another in the older specimens (Fig. 4C). The K14+/K19+ HMECs from the older than 55-year group incorporated 5-fold more EdU than K14+/K19+ cells from the younger than 30-year group ($P < 0.05$; Fig. 4C), and older than 55-year luminal epithelial exhibited a trending increase of EdU incorporation compared with those from women younger than 30 years. That the 3 lineages derived from cKit+ HMEC after only 48 hours of culture exhibited patterns of EdU incorporation similar to the unsorted cells, but without significant differences, suggests that they were proliferating and in an early stage of differentiation (Fig.
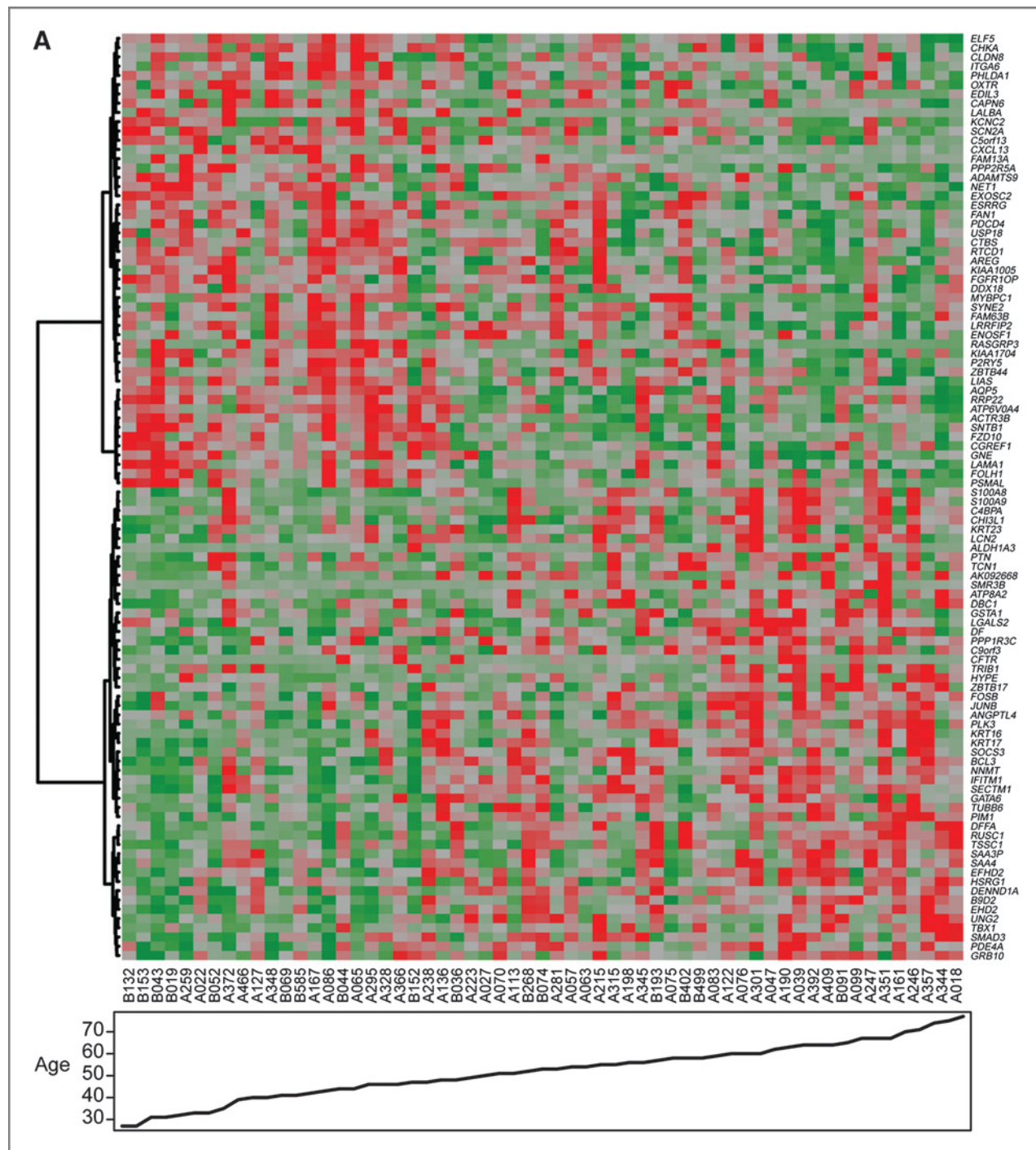
Figure 2. A 100-gene signature stratifies HMECs by age. A, the 100 most variable age-dependent genes identified from a set of 59 LCM phenotypically normal human mammary epithelium samples stratified the gene expression profiles by age.

4C, bottom). That comparable proliferation is exhibited by HMECs with myoepithelial, luminal epithelial, and progenitor phenotypes from women older than 55 years, but not younger than 30 years, may help explain the age-related increase in those populations in strains and organoids.

A small cohort of mammary epithelia exhibit increased basal characteristics with age *in vivo*

To determine the status of keratin expression *in vivo*, K8, K14, and K19 protein expression was evaluated in paraffin-embedded tissue sections of normal breast tissue from 3
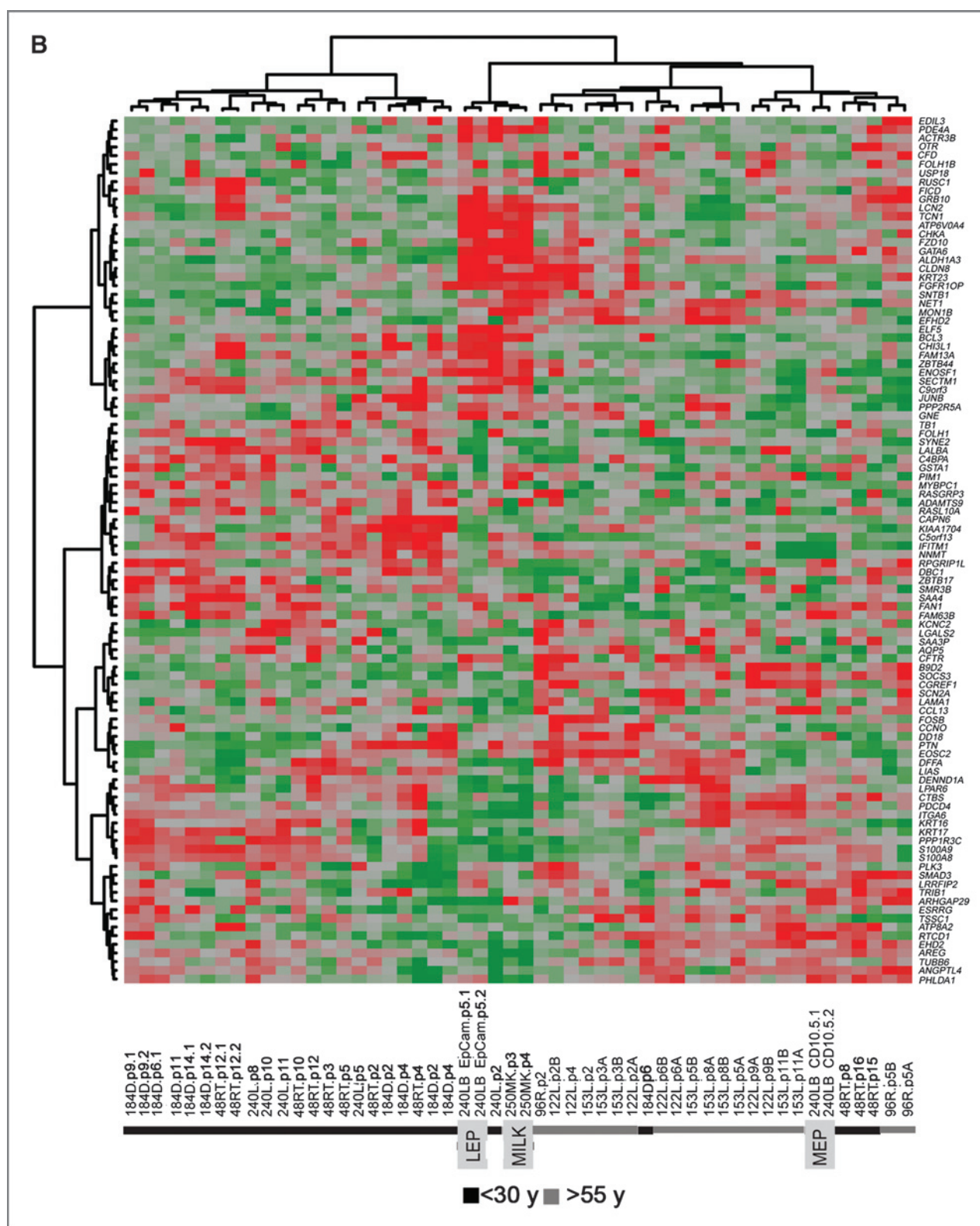
Figure 2. (*Continued*) B, the same signature clustered gene expression profiles of multiple passages and replicates of HMEC strains 184, 48RT, and 240L (<30 years) and 122L, 153, and 96R (>55 years) in an age-dependent manner. Heatmaps represent *z*-scores for each gene, where red represents higher expression and green represents lower expression. A positive fold change represents a higher expression in samples from younger women. Specimen names are shown just below the heatmaps. Profiles from FACS-enriched EpCam⁺ (LEP) and CD10⁺ (MEP) 240L HMEC, and luminal 250MK HMEC from isolated milk (MILK) are indicated. Samples from multiple passages of each HMEC strain are shown (passage is denoted with "p"), and most were analyzed with biologic replicates (denoted either with .1 vs. .2 or A vs. B).
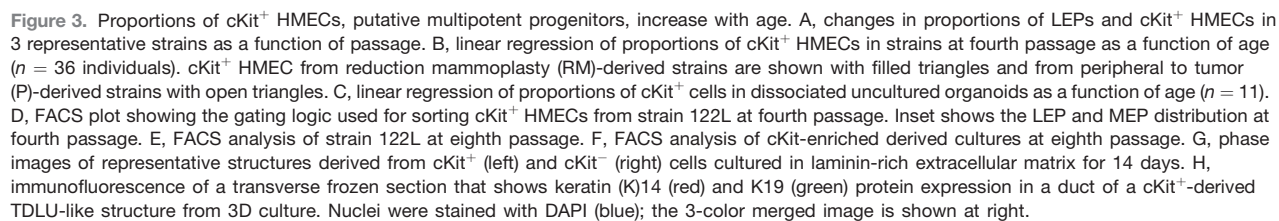
Figure 3. Proportions of cKit[+] HMECs, putative multipotent progenitors, increase with age. A, changes in proportions of LEPs and cKit[+] HMECs in 3 representative strains as a function of passage. B, linear regression of proportions of cKit[+] HMECs in strains at fourth passage as a function of age (n = 36 individuals). cKit[+] HMEC from reduction mammoplasty (RM)-derived strains are shown with filled triangles and from peripheral to tumor (P)-derived strains with open triangles. C, linear regression of proportions of cKit^{+} cells in dissociated uncultured organoids as a function of age (n = 11). D, FACS plot showing the gating logic used for sorting cKit[+] HMECs from strain 122L at fourth passage. Inset shows the LEP and MEP distribution at fourth passage. E, FACS analysis of strain 122L at eighth passage. F, FACS analysis of cKit-enriched derived cultures at eighth passage. G, phase images of representative structures derived from cKit[+] (left) and cKit[−] (right) cells cultured in laminin-rich extracellular matrix for 14 days. H, immunofluorescence of a transverse frozen section that shows keratin (K)14 (red) and K19 (green) protein expression in a duct of a cKit[+]-derived TDLU-like structure from 3D culture. Nuclei were stained with DAPI (blue); the 3-color merged image is shown at right.

Figure 4. cKit$^+$ progenitors exhibit age-dependent differentiation defects. A, a representative contour FACS plot from strain 353P, showing the gating logic used to enrich cKit$^+$ from fourth-passage HMEC strains. B, histograms representing average lineage distributions from 5 individuals younger than 30 years (strains 240L, 407P, 168R, 123, and 124) or 5 older than 55 years (strains 122L, 881P, 353P, 464P, and 451P) in unsorted HMECs (left column) and cKit$^+$ progenitors (right column) after 48 hours of culture on tissue culture plastic. Histograms represent log$_2$-transformed ratios of K14 to K19 protein expression in single cells, histograms are heat mapped to indicate cells with the phenotypes of K14$^-$/K19$^+$ LEPs (green), K14$^+$/K19$^+$ progenitors (yellow), and K14$^+$/K19$^-$ MEPs (red); error bars represent SD ($n = 2,500$ cells/histogram). C, scatter plot representing EdU incorporation in the different lineages, as defined by K14 and K19 expression, in unsorted fourth-passage HMEC strains (top) and cKit$^+$-derived cells (bottom) after 48 hours of culture. Lines indicate average and error bars represent SEM ($n = 2,500$ cells per age group). D, representative images of unsorted, CD227-, and cKit-enriched HMEC from 2 individuals after 48 hours of culture. Protein expression of K14 (red), K19 (green) are shown, and nuclei are stained with DAPI (blue). Scale bar, 20 μm.
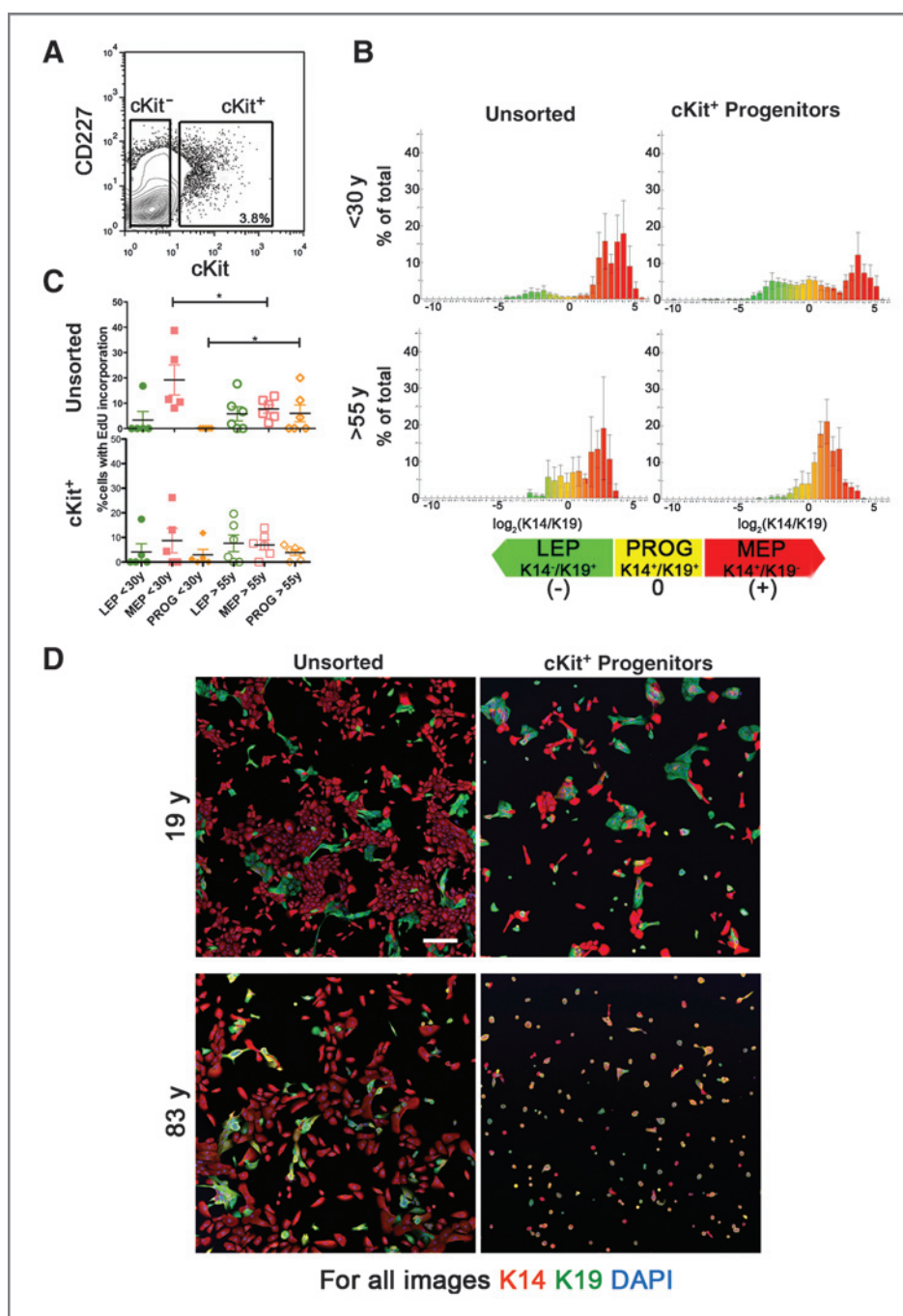
women younger than 45 years and 3 older than 65 years. In addition to markers of lineage, myoepithelials and luminal epithelials can also be identified *in vivo* by their positioning: myoepithelials are adjacent to basement membrane on the basal side of the gland, and luminal epithelial cells are surrounded by myoepithelial cells on the luminal interior side adjacent to the luminal space. Basally located K14-expressing myoepithelials were observed in every specimen (Fig. 5A–D). Luminally located luminal epithelials in the women younger than 45 years expressed more K19 than luminal epithelials in

samples older than 65 years (Fig. 5A and B), whereas there was more K8 expressed in luminal epithelials from the women older than 65 years than in those younger than 45 years (Fig. 5C and D). In the women older than 65 years luminally located luminal epithelial layers exhibited more heterogeneity of K19 expression, with several K19$^-$ cells adjacent to K19$^+$ cells. K14$^+$/K19$^+$ progenitors also appeared more frequently in the samples from women older than 65 years (Fig. 5B, inset). Although qualitative, the samples could be compared with one another because they were stained in parallel and imaged in a single session
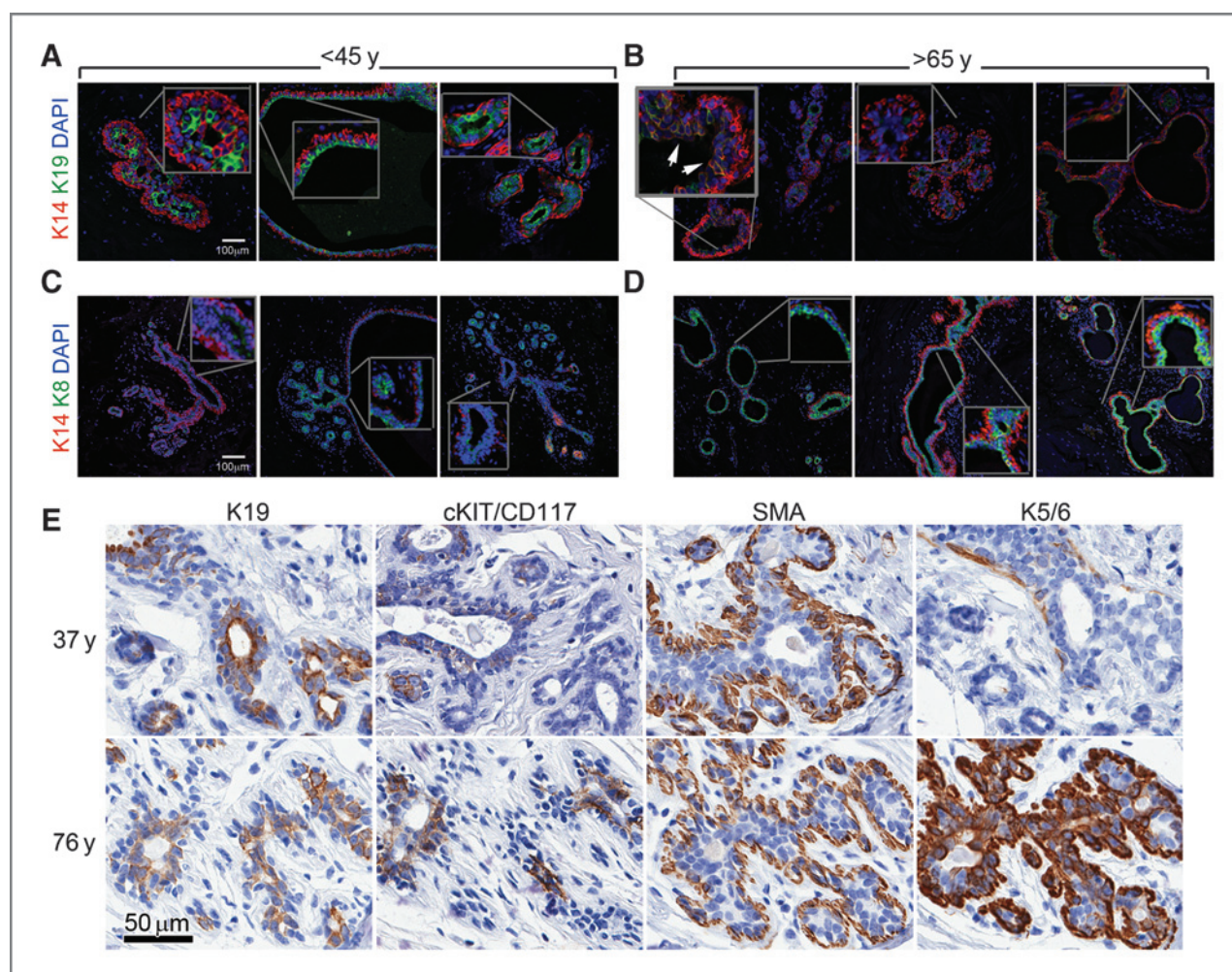
Figure 5. Protein expression patterns *in vivo* are consistent with findings in cultured HMEC strains. Immunofluorescent images of normal mammary glands from 6 individuals from 2 age groups: A and B are stained to show K14 (red) and K19 (green) expression; C and D are stained to show K14 (red) and K8 (green) expression; DAPI nuclear stain shown in all images (blue). Scale bar, 100 μm. Insets show a higher magnification view of the indicated locations within each image, the arrows in B point to 2 clusters of $K14^+/K19^+$ cells. E, four-micrometer serial sections show a lobule from representative 37- and 76-year women immunohistochemically stained to show expression of K19, cKit/CD117, SMA, and K5/6 (brown); nuclei are stained blue. Scale bar, 50 μm.

using the same microscope settings. Moreover, sweat glands within the same sections also stained for K8, K14, and K19, but age-dependent changes in K8 and K19 intensity were not detected (data not shown), thus fixation artifacts were unlikely.

Similar changes were observed in immunohistochemical analysis of 4-μm serial sections from 3 women younger than 45 years and 3 older than 65 years; serial sections that were representative of the analysis are shown from lobules of a 37- and a 76-year woman (Fig. 5E). In the 37-year lobules, K19 was intense and uniformly present in all luminal epithelial and was polarized at the luminal surface, $cKit^+$ cells were infrequent and scattered, myoepithelial marker smooth muscle actin (SMA) was intense in the myoepithelials, and basal keratin K5/6 exhibited light expression in the myoepithelial layer and no expression in luminal epithelials (Fig. 5E, top row). In contrast, the lobule of the 76-year woman showed light K19 expression without polarity in luminal epithelials, strong and

frequent expression of cKit, comparable SMA, and strong K5/6 in luminal epithelials as well as the myoepithelials (Fig. 5E, bottom row). These *in vivo* observations of changes in K19 and K14 expression and the acquisition of more basal phenotypes across the lineages of the mammary epithelium are consistent with the conclusions drawn from the primary and cultured HMEC studies.

Discussion

Aging-related changes to the breast are well known to occur, but their impact on the mammary epithelium and their relationship to the increased frequency of breast cancer in women older than 55 years are not well understood. Molecular signatures of aging at the level of gene expression were reported in human kidney and muscle (38, 39) and now in mammary gland (Fig. 2), which suggests that functionally the

tissues also should differ in young and old. A major challenge that is faced in studying human aging at the cell and molecular levels is the lack of model systems that facilitate a functional understanding of the consequences of molecular changes. We have addressed this problem by using new methodologies that allow long-term growth of HMECs of multiple lineages from women of all ages, enabling examination of normal cell strains in controlled contexts. Culture systems are imperfect replicas of *in vivo*; however, the biochemical and functional phenotypes of aging that were revealed upon examination of the cell strains were corroborated to a large extent by observations of the same phenotypes *in vivo* (e.g., in dissociated uncultured organoids, paraformaldehyde-fixed breast tissue sections, and gene expression from LCM normal breast epithelia).

Functional and molecular interrogation of HMEC strains juxtaposed with analyses of primary organoids and normal breast tissue sections revealed that the proportion of myoepithelials declined, whereas luminal epithelials increased with age. The luminal epithelials from women older than 55 years were surprisingly distinctive compared with their younger counterparts. Through the aging process, luminal epithelials unexpectedly acquired some myoepithelial-like characteristics, which were consistent with age-dependent changes in proportions and activity of cKit$^+$ HMECs. Cultured cKit$^+$ HMEC from women younger than 30 years exhibited functional properties of multipotent progenitors that gave rise to luminal epithelials and myoepithelials, but their activity changed with age, exposing a tendency in cKit$^+$ HMECs from donors older than 55 years to produce luminal epithelials that frequently expressed K14 in addition to K19 and CD227 (Muc1). Myoepithelials derived from cKit$^+$ HMEC of women older than 55 years also exhibited less intense expression of K14 relative to K19, indicating a tendency for the multipotent progenitors to incompletely differentiate into either luminal epithelial or myoepithelial lineages, as they were defined in HMECs from younger women. Importantly, our conclusion that cKit$^+$ HMECs exhibited activity of multipotent progenitors was made possible by functional evaluation of cells enriched from multiple women in both age groups, in addition to the use of organotypic 3D culture and quantitative single-cell analyses of cell fate decisions. The conclusion would potentially have been different had cKit$^+$ HMEC from fewer individuals in only one age group been evaluated. The changes to the epithelium described herein could make older women more vulnerable to malignant progression. Myoepithelial cells are thought to be tumor-suppressive (19, 21), and progenitors are putative etiologic roots of some mammary tumors (22–25). Thus, during the aging process, a putative target population of cells is increased and there is simultaneous decrease in the cells thought to suppress tumorigenic activity.

The factors that lead to the expansion of progenitors are likely to encompass the sum of aging-related changes that occur over an individual's lifespan. For example, endocrine changes from menarche through menopause are well documented and exert system-wide effects. Early menarche and late menopause correlates with increased breast cancer risk (40), as does use of progestin in hormone replacement therapy (41). Dissociated primary human mammary organoids exhibited increased mammosphere-forming units following progesterone exposure, suggesting an increase in multipotent progenitors (42). In mice, progesterone at the luteal diestrus phase (9) and estrogen plus progesterone during pregnancy (8) were shown to cause amplification of the mammary progenitor pool. Perhaps, lifelong repeated hormone exposures during menstrual cycles and pregnancies are the basis for a gradual net gain of cKit$^+$ HMECs.

Age-associated changes to the local breast microenvironment also may account for some of the observed changes in gene expression patterns and lineage distributions. Known age-related changes include increased adipose, decreased connective tissue (15, 17), decreased overall density (16), disruptions in the basement membrane (18), and changes in protease expression (43). These types of changes may alter distributions of the different epithelial lineages because human mammary progenitor cell fate decisions can be influenced by changes in microenvironment (20). In worst case scenarios, extended exposure of mammary epithelia to expression of some matrix metaloproteases lead to outright tumor progression in experimental models (44–46). Embryonic microenvironments (47), and tumor core versus periphery regions (48) were shown to correlate with microenvironment-specific epigenetic modifications to tumor cells. Extending these concepts to normal adult tissues, changes to the breast microenvironment also may help explain age-dependent gene expression patterns and lineage distributions. The fact that an age-dependent gene expression signature persists in early- and late-passage cultured strains argues strongly for metastable epigenetic forms of regulation as important mechanistic components of the age-dependent phenotypes measured here.

Cell culture has a strong selection bias for basal phenotypes, defined here as cells that express CD10, integrins, K14, K5, and bears no markers of luminal epithelials. *In vivo*, the majority of cells with basal phenotypes are located on the basal surface of the gland in contact with the basement membrane. This study was made possible because the *in vitro* basal selection problem was partly solved by using the M87A medium; nevertheless, myoepithelial phenotypes dominated the cultures in late passages regardless of age, indicating that long-term maintenance of the luminal phenotype in culture remains a challenge. The proportional reduction of CD10$^+$ myoepithelials with age is puzzling because cells with basal phenotypes are better able to thrive in ECM-rich microenvironments, such as adjacent to the basement membrane. Moreover, the reduction was obvious by FACS analysis with myoepithelial-specific surface markers in a diverse and large cohort of cultured strains and primary organoids but was difficult to discern in histology sections. It is unlikely that age-related loss of myoepithelials measured by FACS is due to adaptation to culture causing loss of CD10 expression because culture conditions tend to drive more basal phenotypes, and the decrease in myoepithelials was observed in dissociated uncultured organoids. One explanation could be that aging-related loss of lobules (15, 36) created an enrichment of ductal structures, thus the strains established from tissues of older women had an intrinsically different distribution of lineages to begin with. Indeed, analyses of 19 primary organoids by FACS (Figs. 1E and F and 3C) indicated there were

changes in lineage distributions with age in the absence of culture. A second explanation, which is not mutually exclusive with the first, is that the changes in lineage were proportional, and the luminal epithelials and cKit$^+$ progenitors proliferate as well as myoepithelials in HMEC from women older than 55 years, whereas in women younger than 30 years, there was a distinct proliferative advantage in the myoepithelial (Fig. 4C). Finally, the reduction in myoepithelials also could be related to the global changes in gene expression that were observed in the LCM epithelia. Reduced *LAMA1* expression, the α-chain component of laminin-111 that is crucial for normal polarity and is normally expressed by myoepithelials (19, 21), indicated modification of the myoepithelials genetic program. Although uncultured luminal epithelials gained protein expression of integrin-α6 with age, gene expression of integrin-α6 and -β1 was globally reduced with age. Both integrins have been shown to be components of a feedback circuit that regulates the myoepithelial phenotype in mammary epithelial cells from humans and mice (20, 49), suggesting that the basal regulatory machinery may be disrupted in myoepithelials, and inappropriately engaged in luminal epithelials, during the aging process. Use of FACS was emphasized in this study because the technology enabled quantification of lineage distributions in heterogeneous tissues. However, doing so necessitated removing the cells from their *in vivo* context and the small number of histology sections examined did not allow statistical analyses. Thus histology studies of large cohorts of normal breast tissues using the markers described herein will be required to completely reconcile age-related changes that were measured with FACS with histological changes.

The age-dependent epithelial changes described herein, combined with microenvironmental, endocrine, genetic, and epigenetic changes may presage, age-dependent vulnerability to breast cancer. To adequately address, potential preventive and therapeutic interventions, it is important to understand how the aging process is linked to changes in the balance of lineages and to the functioning of progenitors and their progeny and whether there is a direct link between these age-related phenotypes and cancer progression.

Authors' Contributions

Conception and design: A.D. Borowsky, M.A. LaBarge
Development of methodology: J.C. Garbe, F. Pelissier, M. Park, O.W. Petersen, A.D. Borowsky, M.R. Stampfer, M.A. LaBarge
Acquisition of data (provided animals, acquired and managed patients, provided facilities, etc.): J.C. Garbe, F. Pelissier, K. Sputova, A.J. Fridriksdottir, D.E. Guo, R. Villadsen, M. Park, O.W. Petersen, A.D. Borowsky, M.R. Stampfer, M.A. LaBarge
Analysis and interpretation of data (e.g., statistical analysis, biostatistics, computational analysis): J.C. Garbe, F. Pepin, F. Pelissier, D.E. Guo, A.D. Borowsky, M.R. Stampfer, M.A. LaBarge
Writing, review, and/or revision of the manuscript: J.C. Garbe, F. Pepin, A.D. Borowsky, M.R. Stampfer, M.A. LaBarge
Administrative, technical, or material support (i.e., reporting or organizing data, constructing databases): J.C. Garbe, M. Park, M.A. LaBarge
Study supervision: M.A. LaBarge

References

1. DePinho RA. The age of cancer. Nature 2000;408:248–54.
2. Jemal A, Siegel R, Ward E, Murray T, Xu J, Thun MJ, et al. Cancer statistics, 2007. CA Cancer J Clin 2007;57:43–66.
3. Smigal C, Jemal A, Ward E, Cokkinides V, Smith R, Howe HL, et al. Trends in breast cancer by race and ethnicity: update 2006. CA Cancer J Clin 2006;56:168–83.
4. Carey LA, Perou CM, Livasy CA, Dressler LG, Cowan D, Conway K, et al. Race, breast cancer subtypes, and survival in the Carolina Breast Cancer Study. JAMA 2006;295:2492–502.
5. Yau C, Fedele V, Roydasgupta R, Fridlyand J, Hubbard A, Gray JW, et al. Aging impacts transcriptomes but not genomes of hormone-dependent breast cancers. Breast Cancer Res 2007;9:R59.
6. Issa JP, Ottaviano YL, Celano P, Hamilton SR, Davidson NE, Baylin SB, et al. Methylation of the oestrogen receptor CpG island links ageing and neoplasia in human colon. Nat Genet 1994;7:536–40.
7. Waki T, Tamura G, Sato M, Motoyama T. Age-related methylation of tumor suppressor and tumor-related genes: an analysis of autopsy samples. Oncogene 2003;22:4128–33.
8. Asselin-Labat ML, Vaillant F, Sheridan JM, Pal B, Wu D, Simpson ER, et al. Control of mammary stem cell function by steroid hormone signalling. Nature 2010;465:798–802.
9. Joshi PA, Jackson HW, Beristain AG, Di Grappa MA, Mote PA, Clarke CL, et al. Progesterone induces adult mammary stem cell expansion. Nature 2010;465:803–7.
10. Brisken C, Park S, Vass T, Lydon JP, O'Malley BW, Weinberg RA, et al. A paracrine role for the epithelial progesterone receptor in mammary gland development. Proc Natl Acad Sci U S A 1998;95: 5076–81.
11. Lydon JP, DeMayo FJ, Funk CR, Mani SK, Hughes AR, Montgomery CA, et al. Mice lacking progesterone receptor exhibit pleiotropic reproductive abnormalities. Genes Dev 1995;9:2266–78.
12. Mulac-Jericevic B, Lydon JP, DeMayo FJ, Conneely OM. Defective mammary gland morphogenesis in mice lacking the progesterone receptor B isoform. Proc Natl Acad Sci U S A 2003;100:9744–9.
13. Ross RK, Paganini-Hill A, Wan PC, Pike MC. Effect of hormone replacement therapy on breast cancer risk: estrogen versus estrogen plus progestin. J Nat Cancer Inst 2000;92:328–32.
14. Schairer C, Lubin J, Troisi R, Sturgeon S, Brinton L, Hoover R, et al. Menopausal estrogen and estrogen-progestin replacement therapy and breast cancer risk. JAMA 2000;283:485–91.
15. Milanese TR, Hartmann LC, Sellers TA, Frost MH, Vierkant RA, Maloney SD, et al. Age-related lobular involution and risk of breast cancer. J Natl Cancer Inst 2006;98:1600–7.

16. McCormack VA, Perry NM, Vinnicombe SJ, Dos Santos Silva I. Changes and tracking of mammographic density in relation to Pike's model of breast tissue aging: a UK longitudinal study. Int J Cancer 2010;127:452–61.

17. Well D, Yang H, Houseni M, Iruvuri S, Alzeair S, Sansovini M, et al. Age-related structural and metabolic changes in the pelvic reproductive end organs. Semin Nucl Med 2007;37:173–84.

18. Howeedy AA, Virtanen I, Laitinen L, Gould NS, Koukoulis GK, Gould VE. Differential distribution of tenascin in the normal, hyperplastic, and neoplastic breast. Lab Invest 1990;63:798–806.

19. Gudjonsson T, Rønnov-Jessen L, Villadsen R, Rank F, Bissell MJ, Petersen OW. Normal and tumor-derived myoepithelial cells differ in their ability to interact with luminal breast epithelial cells for polarity and basement membrane deposition. J Cell Sci 2002;115:39–50.

20. LaBarge MA, Nelson CM, Villadsen R, Fridriksdottir A, Ruth JR, Stampfer MR, et al. Human mammary progenitor cell fate decisions are products of interactions with combinatorial microenvironments. Integr Biol 2009;1:70–9.

21. Hu M, Yao J, Carroll DK, Weremowicz S, Chen H, Carrasco D, et al. Regulation of in situ to invasive breast carcinoma transition. Cancer Cell 2008;13:394–406.

22. Lim E, Vaillant F, Wu D, Forrest NC, Pal B, Hart AH, et al. Aberrant luminal progenitors as the candidate target population for basal tumor development in BRCA1 mutation carriers. Nat Med 2009;15:907–13.

23. Molyneux G, Geyer FC, Magnay FA, McCarthy A, Kendrick H, Natrajan R, et al. BRCA1 basal-like breast cancers originate from luminal epithelial progenitors and not from basal stem cells. Cell Stem Cell 2010;7:403–17.

24. Proia TA, Keller PJ, Gupta PB, Klebba I, Jones AD, Sedic M, et al. Genetic predisposition directs breast cancer phenotype by dictating progenitor cell fate. Cell Stem Cell 2011;8:149–63.

25. Kouros-Mehr H, Bechis SK, Slorach EM, Littlepage LE, Egeblad M, Ewald AJ, et al. GATA-3 links tumor differentiation and dissemination in a luminal breast cancer model. Cancer Cell 2008;13:141–52.

26. Stampfer M, Hallowes RC, Hackett AJ. Growth of normal human mammary cells in culture. In Vitro 1980;16:415–25.

27. Garbe JC, Bhattacharya S, Merchant B, Bassett E, Swisshelm K, Feiler HS, et al. Molecular distinctions between stasis and telomere attrition senescence barriers shown by long-term culture of normal human mammary epithelial cells. Cancer Res 2009;69:7557–68.

28. Finak G, Sadekova S, Pepin F, Hallett M, Meterissian S, Halwani F, et al. Gene expression signatures of morphologically normal breast tissue identify basal-like tumors. Breast Cancer Res 2006;8:R58.

29. Smyth GK. Limma: linear models for microarray data. In:Gentleman R, Carey V, Dudoit S, Irizarry R, Huber W, editors. Bioinformatics and computational biology solutions using R and bioconductor. New York: Springer; 2005. p. 397–420.

30. Benjamini Y, Hochberg Y. Controlling the false discovery rate: a practical and powerful approach to multiple testing. J R Stat Soc Ser 1995;57:289–300.

31. Taylor-Papadimitriou J, Stampfer M, Bartek J, Lewis A, Boshell M, Lane EB, et al. Keratin expression in human mammary epithelial cells cultured from normal and malignant tissue: relation to in vivo phenotypes and influence of medium. J Cell Sci 1989;94:403–13.

32. Brenner AJ, Stampfer MR, Aldaz CM. Increased p16 expression with first senescence arrest in human mammary epithelial cells and extended growth capacity with p16 inactivation. Oncogene 1998;17:199–205.

33. Raouf A, Zhao Y, To K, Stingl J, Delaney A, Barbara M, et al. Transcriptome analysis of the normal human mammary cell commitment and differentiation process. Cell Stem Cell 2008;3:109–18.

34. Gudjonsson T, Villadsen R, Nielsen HL, Rønnov-Jessen L, Bissell MJ, Petersen OW. Isolation, immortalization, and characterization of a human breast epithelial cell line with stem cell properties. Genes Dev 2002;16:693–706.

35. Villadsen R, Fridriksdottir AJ, Rønnov-Jessen L, Gudjonsson T, Rank F, LaBarge MA, et al. Evidence for a stem cell hierarchy in the adult human breast. J Cell Biol 2007;177:87–101.

36. Hutson SW, Cowen PN, Bird CC. Morphometric studies of age related changes in normal human breast and their significance for evolution of mammary cancer. J Clin Pathol 1985;38:281–7.

37. Regan JL, Kendrick H, Magnay FA, Vafaizadeh V, Groner B, Smalley MJ. c-Kit is required for growth and survival of the cells of origin of Brca1-mutation-associated breast cancer. Oncogene 2012;31:869–83.

38. Rodwell GE, Sonu R, Zahn JM, Lund J, Wilhelmy J, Wang L, et al. A transcriptional profile of aging in the human kidney. PLoS Biol 2004;2:e427.

39. Zahn JM, Sonu R, Vogel H, Crane E, Mazan-Mamczarz K, Rabkin R, et al. Transcriptional profiling of aging in human muscle reveals a common aging signature. PLoS Genet 2006;2:e115.

40. Bernstein L. Epidemiology of endocrine-related risk factors for breast cancer. J Mammary Gland Biol Neoplasia 2002;7:3–15.

41. Rossouw JE, Anderson GL, Prentice RL, LaCroix AZ, Kooperberg C, Stefanick ML, et al. Risks and benefits of estrogen plus progestin in healthy postmenopausal women: principal results From the Women's Health Initiative randomized controlled trial. JAMA 2002;288:321–33.

42. Graham JD, Mote PA, Salagame U, van Dijk JH, Balleine RL, Huschtscha LI, et al. DNA replication licensing and progenitor numbers are increased by progesterone in normal human breast. Endocrinology 2009;150:3318–26.

43. Imai S, Nishibayashi S, Takao K, Tomifuji M, Fujino T, Hasegawa M, et al. Dissociation of Oct-1 from the nuclear peripheral structure induces the cellular aging-associated collagenase gene expression. Mol Biol Cell 1997;8:2407–19.

44. Sternlicht MD, Lochter A, Sympson CJ, Huey B, Rougier JP, Gray JW, et al. The stromal proteinase MMP3/stromelysin-1 promotes mammary carcinogenesis. Cell 1999;98:137–46.

45. Radisky DC, Levy DD, Littlepage LE, Liu H, Nelson CM, Fata JE, et al. Rac1b and reactive oxygen species mediate MMP-3-induced EMT and genomic instability. Nature 2005;436:123–7.

46. Sternlicht MD, Bissell MJ, Werb Z. The matrix metalloproteinase stromelysin-1 acts as a natural mammary tumor promoter. Oncogene 2000;19:1102–13.

47. Costa FF, Seftor EA, Bischof JM, Kirschmann DA, Strizzi L, Arndt K, et al. Epigenetically reprogramming metastatic tumor cells with an embryonic microenvironment. Epigenomics 2009;1:387–398.

48. Jie G, Zhixiang S, Lei S, Hesheng L, Xiaojun T. Relationship between expression and methylation status of p16INK4a and the proliferative activity of different areas' tumour cells in human colorectal cancer. Int J Clin Pract 2007;61:1523–9.

49. Deugnier MA, Faraldo MM, Rousselle P, Thiery JP, Glukhova MA. Cell-extracellular matrix interactions and EGF are important regulators of the basal mammary epithelial cell phenotype. J Cell Sci 1999;112:1035–44.